



Investigation of Structural Changes during the Recovery of Crystal Defects in: Laser Damaged Fe₅₀Ni₅₀ Alloy by Magnetic Measurements

Ali AR, Takla E, Meleka KK

Physics Department, Faculty of Science, Cairo University, Giza, Egypt

Abstract Using magnetic measurements, the behavior of structural changes induced by annealing out of quenched - in vacancies in ordered Fe₅₀Ni₅₀ alloy (L1₂) type structure. The observed increase in magnetic permeability with increasing quenching temperature ($450 > T_q > 650$ °C) was attributed to the increase in the total number of mobile domain walls due to the reduction in the density of pinning sites in the alloy matrix. On the other hand, the influence of quenching from different temperatures on the magnetic anisotropy was attributed to the increase in the internal microstress in the alloy matrix by successive pre-quenching from different temperatures. The isochronal annealing of quenched samples in the temperature range from 325 to 500 °C (stage I) revealed a decrease in the maximum permeability during annealing, and was attributed to the short-range order caused by the long- range migration of quenched-induced defects. The second annealing stage appearing in the temperature range from 500 to 700 °C is associated with an increase in μ_{max} due to the dissociation of vacancy clusters or complex aggregates formed during (stage I) or after quenching treatment, resulting in a release of free mono- vacancies. The determined activation energy for vacancy formation (1.67 ± 0.01 eV) has the same order of magnitude as that required for Fe and Ni alloy. The recovery stage in the temperature range from 700 to 800 °C (stage III) appears only in cold-worked samples was attributed to the recovery process of dislocations during the recrystallization process.

Keywords Fe₅₀Ni₅₀ - ferromagnetic alloy - magnetic properties – quenching - vacancy formation

Introduction

Stainless steel, Fe-based and permalloy alloys are an important class of materials for present and future technological applications [1-9]. Actually, the structure sensitive properties of these materials are directly dependent on such fundamental processes as creation of lattice defects, defect diffusion, and defect reaction in the alloy matrix. On the other hand, the changes in the structural sensitive properties of Fe-based alloys have been observed by several authors [10-12] during the annealing of irradiated or cold-worked alloys above room temperature. Results of some of those experiments have been explained on the basis of either solute segregation, changes in short-range order or precipitation of ordered phases. These processes cause microscopic homogeneities in the alloy matrix which lead to anomalous changes in the physical property measured. Moreover, the present binary alloy Fe₅₀Ni₅₀ of superstructure L1₂ type (Ni₃Fe) [13], its prospect as soft magnetic material and good corrosion resistance [14,15] at elevated temperature are of additional interest. This binary system forms a long range ordered intermetallic phase with superstructure L1₂ type (Ni₃Fe), which has FCC unit cell with Fe atoms occupy the corners and Ni atoms occupy the middle of the faces of the cube [16], while in the disordered phase, Ni and Fe atoms randomly occupy the FCC lattice sites. According to the constitution diagram of Fe-Ni alloy [16] the ordered and disordered phases coexist in equilibrium around 830 K, while below this temperature the ordered phase is stable. Moreover, in this class of intermetallic materials, unlike in pure metals or solid solution alloys, there exists a restriction imposed on the formation and movements of vacancies. This restriction is due to the thermal formation of vacancies on the two sublattices, concomitant thermal formation of antisite defects on both sublattices, and the coexistence of point defects due to deviations from the stoichiometric composition [17,18]. Therefore, it is expected that the annealing behavior of the physical parameters of intermetallic compounds after quenching are more complex than in pure metals. On the other hand, since in intermetallic compounds the local order transformation caused by short-range or long-range



ordering are induced by diffusion of point defects. Therefore, it is difficult to separate ordering effects from those due to vacancy or interstitial annealing. Although several studies [18-20] have been made on the thermal formation and migration of point defects in intermetallic compounds by various techniques, fundamental information on the temperature and composition dependence of point defects is still remains a challenging problem. The magnetic structure sensitive properties measured in this work, such as the maximum magnetic permeability (μ_{\max}) and the magnetic coercivity (M_{cr}) are highly defect specific and it can be used to study the formation sequence and relative stability of corresponding microstructure configuration in intermetallic $\text{Fe}_{50}\text{Ni}_{50}$ alloy.

The aim of the present work is to study the behavior of structural changes induced by lattice defects created in intermetallic compound $\text{Fe}_{50}\text{Ni}_{50}$, during and after quenching and also to study the influence of additional lattice defects produced by plastic deformation on the behavior of isochronal annealing of quenched $\text{Fe}_{50}\text{Ni}_{50}$ alloy.

Experimental Work

The test material, $\text{Fe}_{50}\text{Ni}_{50}$ alloy, was prepared from high purity Fe and Ni by induction melting followed by a suitable homogenization at 1200 °C under a helium atmosphere for 24 hours, then slowly cooled to room temperature. The material shaped by extrusion into rods of 3 mm diameter followed by swaging at room temperature to wires of 1 mm diameter .

The atomic absorption method was used in order to determine the composition of the alloy (Table 1) [21]. The wire sample was introduced as the core of a magnetization coil and the cathode ray technique was employed to obtain room-temperature B-H curves at different magnetizing fields. The maximum magnetic permeability was obtained from the relation: $\mu_{\max} = (B/H)_{\max}$, which characterizes the magnetization of both reversible and irreversible domain-wall motion. Plastic strain deformation was induced on the samples by a locally conventional strain machine. The different degrees of plastic strain deformation were measured by the dimensionless quantity: $\eta\% = [(\Delta L/L) \times 100]$, where ΔL and L are the change in length and the initial length of the sample respectively [22].

A cylindrical non-inductive furnace of length 30 cm and diameter 9 cm with heater wire uniformly distributed along its length was used. A silica glass tube was inserted containing the specimen, and the temperature inside the furnace was constant along its middle third of its length and could be maintained constant for several hours to within ± 2 °C. After giving the samples prescribed annealing pulses the silica tube container was taken out from the furnace and left in air to cool to room temperature. Isochronal annealing was used to study the structural changes during recovery of plastically deformed of $\text{Fe}_{50}\text{Ni}_{50}$ alloy. In isochronal annealing, the sample was heated for a constant time at different increasing temperatures. Care was taken during cooling from the curve annealing temperature and in the subsequent reheating to control the rate of temperature changes, so that it was never so great to cause further plastic deformation. The quenching is performed by holding the specimen at 900 °C then quenched in cold water with rate of quenching 3×10^3 K/s.

Table 1: Chemical composition of $\text{Fe}_{50}\text{Ni}_{50}$ alloy.

Fe	Ni	Mn	Zn	Mg	Sn	Al	Cu
Major	Major	-	0.001	-	0.001	0.001	0.001

Results

Effect of Pre-Quenching on μ_{\max} and H_{cr} :

The magnetic permeability (μ) measured at room temperature as a function of the magnetizing field (H) after pre-quenching from different temperatures for $\text{Fe}_{50}\text{Ni}_{50}$ alloy is presented in Fig. 1. The curves are characterized by pronounced peak values in the maximum magnetic permeability (μ_{\max}). These peaks shifted their positions to higher or lower magnetic fields depending on the quenching temperatures. The dependence of both the relative changes in quenched-maximum magnetic permeability $(\Delta\mu_{\max})_q$ and critical magnetic field $(\Delta H_{\text{cr}})_q$ on the quenching temperatures is illustrated in Figure 2. The general behaviour noticed in the present study is the initial increase of $(\Delta\mu_{\max})_q$ with quenched temperature up to a maximum obtained at $T_q = 600$ °C, beyond which it decreases leading to maximum permeability values smaller than that measured before quenching treatment. Meanwhile, the relative changes in critical magnetic field initially decreased followed by a pronounced increase after the same quenching treatment (Fig. 2).



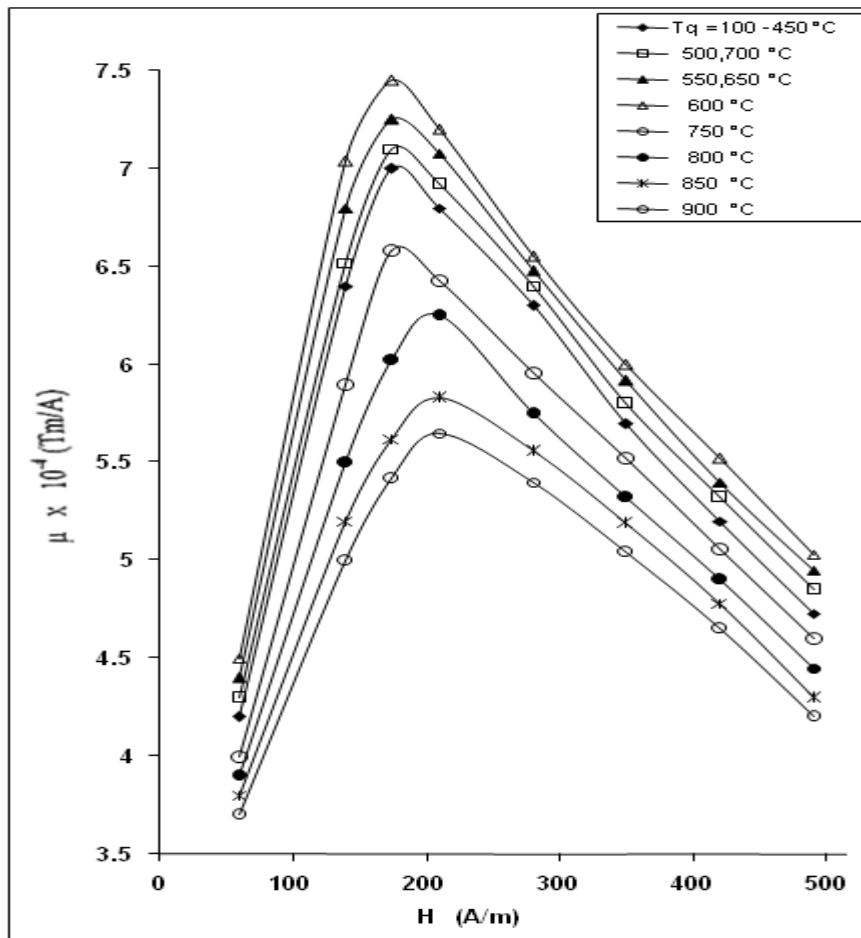


Figure 1: The dependence of magnetic permeability (μ) on the magnetic field (H) for quenched $Fe_{50}Ni_{50}$ alloy for different annealing temperatures.

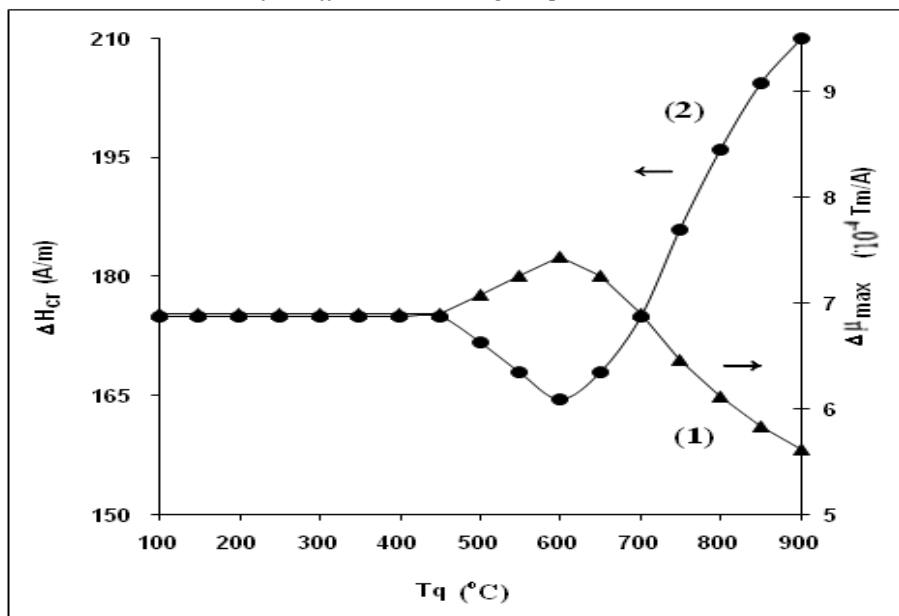


Figure 2: Dependence of the relative change in maximum magnetic permeability ($\Delta\mu_{max}$) and critical magnetic field (ΔH_{cr}) on the quenching temperature (T_q) for $Fe_{50}Ni_{50}$ alloy.

Activation energy for vacancy formation in Fe₅₀Ni₅₀ alloys:

It is now well accepted that the change in structure ordering by short range order in Fe₅₀Ni₅₀ type L1₂ is controlled by vacancy formation and migration above room temperature [12,23]. Therefore, in the present work, it is reasonable to find the formation energy of vacancy in Fe₅₀Ni₅₀ alloy. The apparent vacancy formation energy in quenched alloy was calculated based on the relative change in the maximum magnetic permeability ($\Delta\mu_{\max}$)_q, critical magnetic field (ΔH_{cr})_q (Fig. 3). The obtained value of energy (1.67 ± 0.01 eV), is in close agreement with the other reported value of free vacancies formation in similar intermetallic compounds [12,24]. This value of activation energy suggested that most vacancies formed in quenched Fe₅₀Ni₅₀ alloy, (quenched from temperatures $600 < T_q < 800$ °C), are free vacancies predominantly exist on Ni sublattice together with a concentration of antisite atoms on both sublattices of the alloy matrix [17]. The deviated points from the straight line (see Figure 3), implies that a complex structure of vacancies or precipitated phase was formed during quenching from higher temperature ($T_q > 750$ °C). Increasing the quenching temperature above 750 °C increases both the concentration of vacancy aggregates and the amount of precipitation in the quenched matrix.

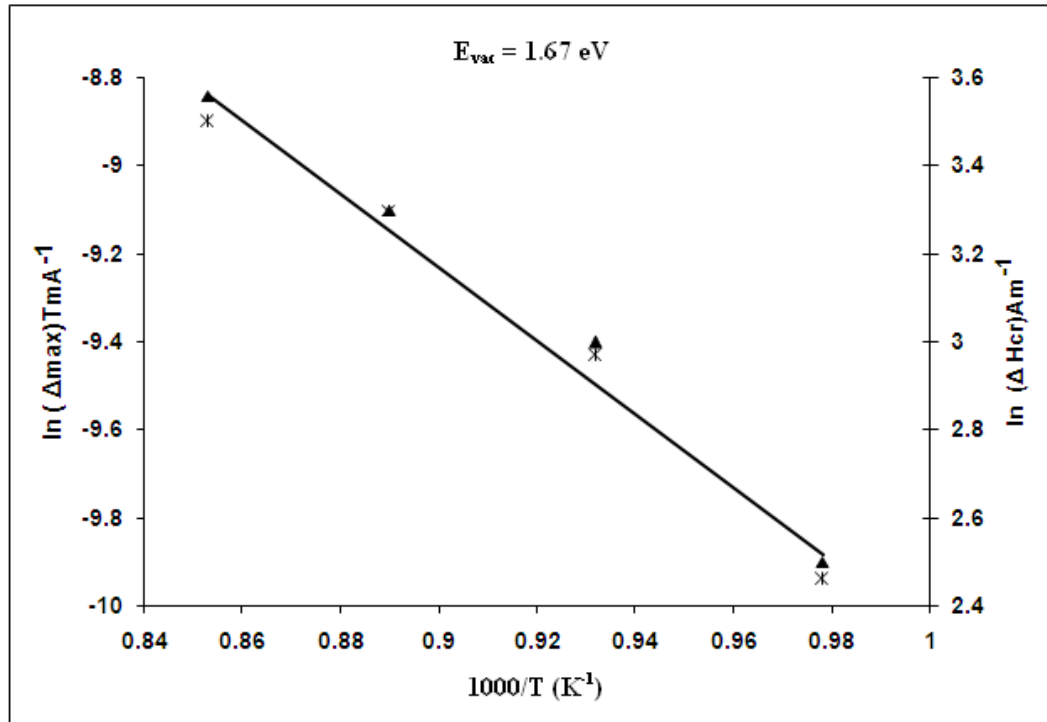


Figure 3: Dependence of the apparent formation energy of vacancies in the Fe₅₀Ni₅₀ alloy from the relative change in the maximum magnetic permeability [$\Delta\mu_{\max}$ (▲)] and the critical magnetic field [ΔH_{cr} (×)].

Isochronal Annealing of Quenched Fe₅₀Ni₅₀ Alloy:

Room temperature changes of the magnetic permeability of Fe₅₀Ni₅₀ alloy were traced after isochronal annealing of quenched sample ($T_q = 900$ °C), with the quenching rate 3×10^3 k/s by heat pulses of 10 min at temperatures successively increased in steps of 25 K (Fig. 4). The results have been reported in normalized form of maximum magnetic permeability namely, the fraction K_{norm} has been used and is given by:

$$K_{norm} = \frac{[\mu_{\max}(T_a) - \mu_{\max}(q)]}{[\mu_{\max}(f) - \mu_{\max}(q)]} = \frac{\Delta\mu_{\max}(T_a)}{\Delta\mu_{\max}(0)} \quad (1)$$

where $\mu_{\max}(q)$ is the value of the maximum magnetic permeability of quenched sample before annealing, $\mu_{\max}(T_a)$ and $\mu_{\max}(f)$ are the values after annealing temperature (T_a) and after final temperature anneal, respectively.

The relative changes in the maximum magnetic permeability and the observed annealing spectrum of quenched Fe₅₀Ni₅₀ alloy in the temperature range from 25 to 900 °C are represented in Fig. 5 and Fig. 6. It revealed the presence of two annealing stages. Stage I shows itself as a decrease in the maximum permeability with the annealing temperature in temperature range from 325 to 500 °C, while stage II shows itself as increase in the maximum magnetic permeability (μ_{\max}) in temperature range from 525 to 675 °C. A final decrease in the maximum magnetic permeability is observed above 650 °C.



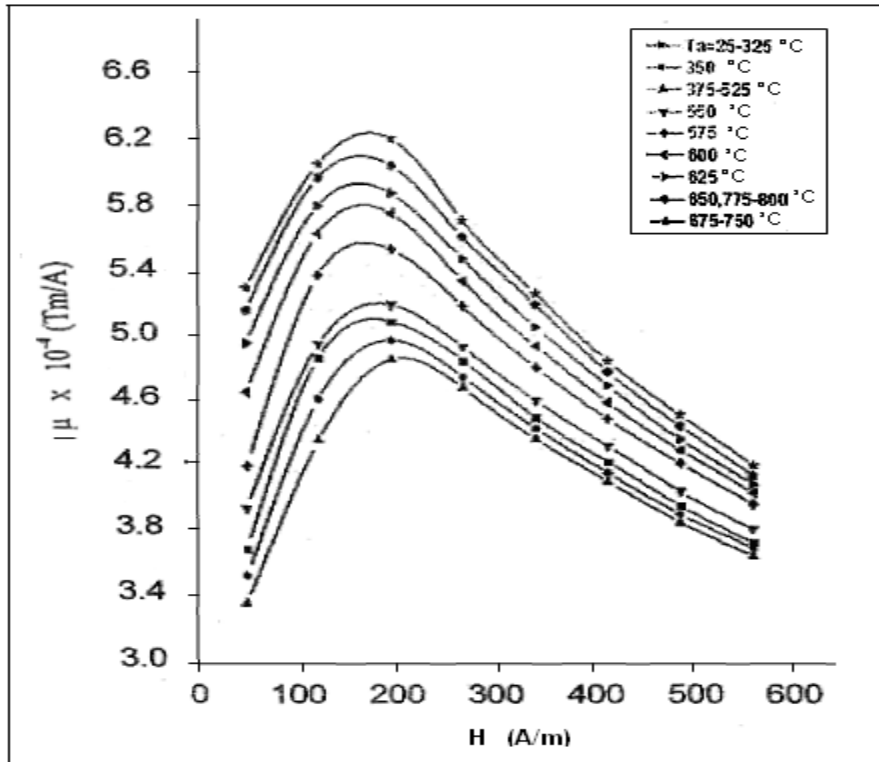


Figure 4: The effect of isochronal annealing temperature on the dependence of the magnetic permeability, μ on the magnetic field, H of quenched $Fe_{50}Ni_{50}$ alloy ($T_q = 900^\circ C$).

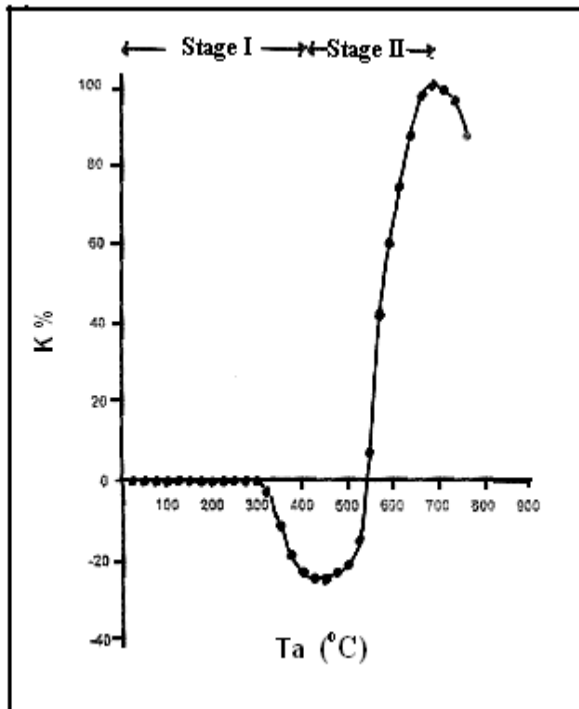


Figure 5: Relative change in the maximum magnetic permeability ($K\%$) of quenched $Fe_{50}Ni_{50}$ sample ($T_q = 900^\circ C$) with the annealing temperature.

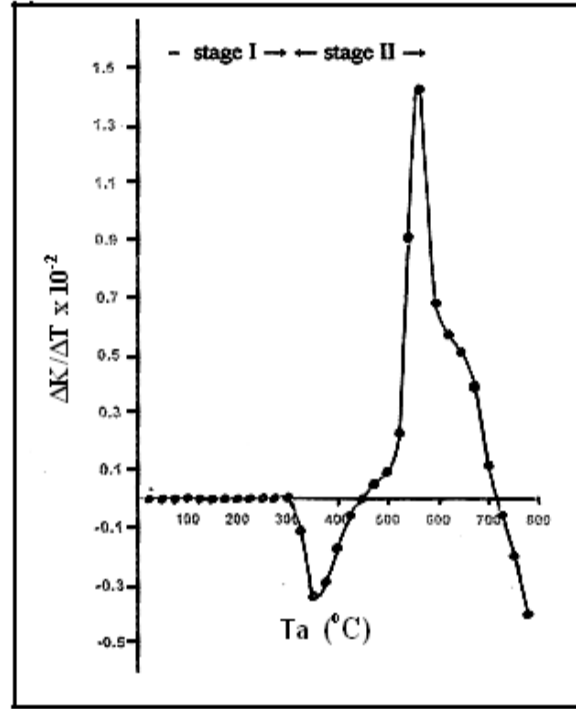


Figure 6: The spectrum of quenched $Fe_{50}Ni_{50}$ sample ($T_q = 900^\circ C$) with the annealing temperature.

Influence of Plastic Strain after Quenching on the Behavior of Recovery of Fe₅₀Ni₅₀ Alloy:

To study the influence of additional lattice defects produced by plastic deformation on the behavior of isochronal annealing of quenched Fe₅₀Ni₅₀ alloy, it is desirable to carry out isochronal annealing of a sample plastically strained after quenching from higher temperatures ($T_q = 900\text{ }^\circ\text{C}$). It is seen that the additional lattice defects produced by plastic strain in quenched sample modifies the relative change in the maximum permeability during isochronal annealing. It is also noticed that the amplitude of stages I and II becomes smaller and the position of stage I shifted towards lower annealing temperature, while the position of stage II shifted towards higher temperature (Fig. 8). Moreover, an additional third annealing stage (stage III) shows itself in the temperature range from 725 to 800 °C, appeared only for a sample plastically strained after quenched, while the final decrease in the maximum permeability is observed above 800 °C (Fig. 7 and Fig. 8).

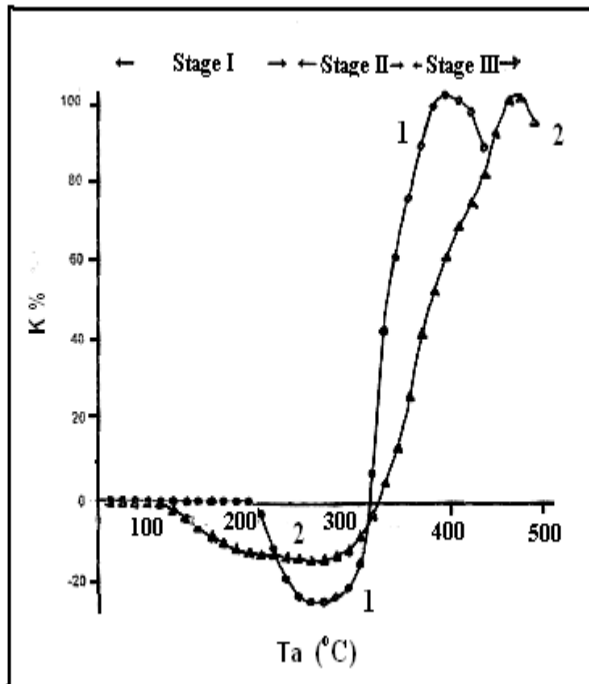


Figure 7: Relative change in the maximum magnetic permeability ($K\%$) of: (1) quenched Fe₅₀Ni₅₀ sample ($T_q = 900\text{ }^\circ\text{C}$), and (2) strained pre-quenched Fe₅₀Ni₅₀ sample with the annealing temperature.

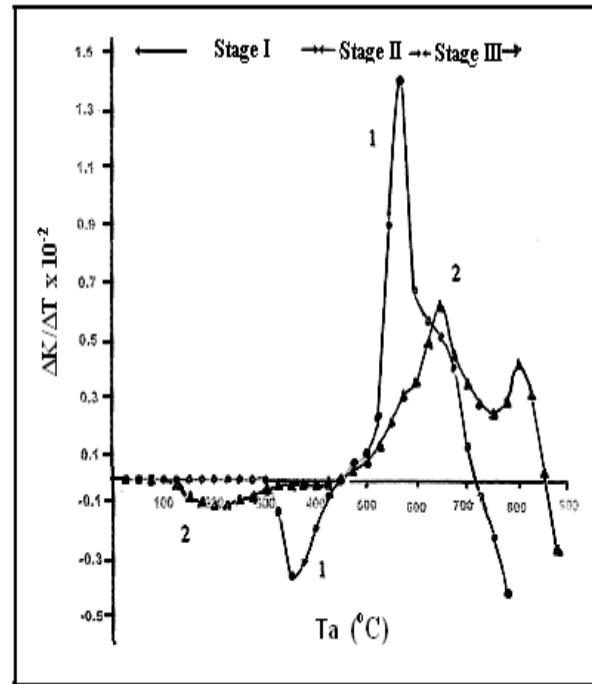


Figure 8: Spectrum diagram of the maximum magnetic permeability ($K\%$) of: (1) quenched Fe₅₀Ni₅₀ sample ($T_q = 900\text{ }^\circ\text{C}$), and (2) strained pre-quenched Fe₅₀Ni₅₀ sample with the annealing temperature.

Discussion and Conclusion:

The results of the isochronal annealing observed in the present work of quenched Fe₅₀Ni₅₀ alloy, in the temperature range from 125 to 900 °C (Fig. 6 and Fig. 8) are quite different from those previously reported for quenched α -Fe [25,26] and some Fe-alloys [26,27]. In the present work, the anomalous change in μ_{\max} and H_{cr} in the temperature range 125-500 °C (stage I) could not be described to the annihilation of lattice defects induced by quenched alone. It could be explained on the basis of either solute segregation, changes in short-range order, or precipitation of ordered phase [28,29]. The above processes cause microscopic inhomogeneities leading to an increase in the internal stress in the alloy matrix [30]. This was expected to increase the density of pinning sites for the motion of magnetic domain walls in the matrix, resulting in the increase of H_{cr} and the decrease of μ_{\max} beyond the pre-annealed value (Fig. 6 and Fig. 8). Beside, the structural change by short-range order has been assigned by most workers to the migration of either self-interstitial atoms as well as that of vacancies [12,28]. In the present work, since the isochronal annealing during stage I is continued over the whole temperature range from 125 to 500 °C, therefore, the interstitial atoms migration could be definitely excluded in this temperature range [31]. From this consideration stage I could be attributed the structural change in the alloy matrix by short-range ordering promoted by migration of vacancies, formed by plastic deformation and quenching Fe₅₀Ni₅₀ alloy to deep traps or sinks. During isochronal annealing of the disordered Fe₅₀Ni₅₀ alloy of structure below equilibrium level each vacancy jump induced a certain increase of local order. This corresponds to a decrease in μ_{\max} and an increase in H_{cr} . The contribution of vacancy migration, leading to an increase in short-



range order, has also been suggested by Sharma et al. [32] and Nakata et al. [33] in annealing studies of irradiated Fe-Cr-Ni alloy. These evidences suggest that in the present stage (stage I) the anomalous change in μ_{\max} and H_{cr} is due to the change in the local order produced by the long-range migration of vacancies. When the vacancy become mobile, it performs a certain number of jumps before annihilation or trapping in clusters and can promote the evolution of the local atomic order of the alloy towards its equilibrium state. These results support the idea that the change in structural ordering by short-range order is controlled by free vacancy migration, with the possible formation of vacancy clusters or complex aggregates [25,26]. The second annealing stage (stage II) centered around 600 °C, showing up as an increase in μ_{\max} is associated with a decrease in H_{cr} . This annealing stage observed in the present work in quenched and pre-strained quenched samples (see Fig. 6 and Fig. 8) could be attributed to the dissociation of vacancy clusters or complex aggregates formed during stage I or after quenching, resulting in a release of free mono-vacancy. The vacancy migrates further to a deeper trap or falls into sinks during the migration process with annealing temperature rising from 550 to 750 °C. This process was expected to decrease the density of the load on the magnetic domain walls. Hence an increase in μ_{\max} together with a drop in H_{cr} was observed during this annealing stage (see (Fig. 6 and Fig. 8).

The higher temperature annealing stage (stage III) observed in the present work only during the isochronal annealing of pre-strained quenched Fe₅₀Ni₅₀ alloy in the temperature range from 750 to 825 °C could be attributed to a recrystallization phenomenon (see Fig. 8). The observed increase of μ_{\max} , when recrystallization started in the deformed alloy matrix, was thought to be due to the release of some of the dislocations forming the cell boundaries through a process of climb by edge dislocation [34]. The subsequent removal of these dislocations settles down the density of pinning sites for the motion of magnetic domain walls in the matrix, which consequently decrease the load on the magnetic domain. Hence a continuous decrease in H_{cr} associated with an increase in μ_{\max} was observed in this annealing stage (see Fig. 8). Moreover, the value of the activation energy ($E_m^v = 1.19 \pm 0.01$ eV) obtained as the mean migration energy of vacancies in the present work, could added to the value of formation energy ($E_f^v = 1.65 \pm 0.02$ eV) obtained also in the present work (see Fig. 4). The sum is (2.84 ± 0.03 eV) which in good agreement with the activation energy of self-diffusion mechanism in Ni-based L1₂ type intermetallic compound.

Finally, we come now to the observed decrease in the maximum magnetic permeability in quenched and pre-strained quenched samples in the temperature range from 825 to 900 °C (see Fig. 8). This decrease is most probably due to the precipitation of FeNi₃ phase [35,36]. The precipitation of this phase causes a marked expansion of the material, leading to an increase in the dislocation density in the alloy matrix [35, 36]. This process seemed to impose a heavily pinning action on the magnetic domain walls, preventing them from normal attachment from fixation points and leak out the magnetic pressure exerted by the magnetic field on domain walls [26,37].

Acknowledgement

The authors would like to express their appreciations to *Dr. Fahmy Z. Ghobrial*, Physics Department, Faculty of Science, Cairo University, Giza, Egypt, *for spiritual support and maternal care he provided throughout the whole work and during the preparation of this manuscript.*

References

- [1]. Shihong Shi, Aiqin Xu, Jiwei Fan, & Hongpu Wei (2012). *Nuclear Engineering and Design*, 245:8.
- [2]. Li, H. M., Sun, D. Q., Cai, X. L., & Wang, W. Q. (2012). *Materials and Design*, 39:285.
- [3]. Baicheng Zhang, Nour-Eddine Fenineche, Lin Zhu, Hanlin Liao, & Christian Coddet, (2012). *Journal of Magnetic Materials*, 324:495.
- [4]. Ebrahimzadeh, H., & Mousavi, S. A. A. (2012). *Materials and Design*, 38:115.
- [5]. Gupta, K., Raina, K. K., & Sinha, S. K. (2007). *Journal of Alloys and Compounds*, 429:357.
- [6]. Dudarev, S. L., & Derlet, P. M. (2007). *Journal of Nuclear Materials*, 367-370:251.
- [7]. Jacques Dalla Torre, Chu-Chun Fu, Francois Willaiame, Alian Barbu, & Jean-Louis Bocquet (2006). *Journal of Nuclear Materials*, 352:42.
- [8]. Chu-Chun Fu, Jacques Dalla Torre, Francois Willaiame, Jean-Louis Bocquet, Alian Barbu (2005). *Nature Materials*, 4:68.
- [9]. Vicente Alvarez, M. A., Marchina, M., & Perez, T. (2008). *Metallurgical and Materials Transactions A*, 39:3283.
- [10]. Dimitrov, C., Huguenin, D., Moser, P., & Dimitrov, O. (1990). *Journal of Nuclear Materials*, 147:22.



- [11]. Ghazi-Wakili, K., Tipping, Ph., Zimmermann, U., & Waeber, W. B. (1990). *Z. Phys. B Condensed Matter*, 79, 39 (1990).
- [12]. Anand, M. S., & Pande, B. M. (1994). *Phys. Stat. Sol. (a)*, 144:285.
- [13]. Lima, E. Jr., & Drago, V. (2004). *Journal of Magnetism and Magnetic Materials*, 280:251.
- [14]. Coutu, L., Chaput, L., & Waekerle, T. (2000). *Journal of Magnetism and Magnetic Materials*, 215-216:237.
- [15]. Wurschum, R., Kummeler, E. A., Badura-Gergen, K., & Schaefer, H. E. (1996). *Appl. Phys.*, 80:724.
- [16]. Sumiayma, K. (1991). *Phys. Stat. Sol. (a)*, 126, 291 (1991).
- [17]. Brossmann, U., Wurschum, R., Badura-Gergen, K., & H.E.Schaefer, H. E. (1994). *Phys. Rev. B*, 49(10):6457.
- [18]. Schaefer, H. E., Wurschum, R., & Bub, J. (1992). *Mater. Sci. Forum.*, 105:110.
- [19]. Schaefer, H. E., Damson, B., Weller, M., Arzt, E., & George, E. P. (1997). *Phys. Stat. Sol. (a)*, 160:531.
- [20]. Chang, Y. A., Pike, L. M., Liu, C. T., Bilbrey, A. R., & Stone, D. S. (1993). *J. Intermetal.*, 1:107.
- [21]. Ali, A. R., Ghobrial, F. Z., Takla, E., & Meleka, K. K. (2015). *Materials Science*, 13(3):108.
- [22]. Gorkunov, E. S., Zadvorkin, S. M., Smirnov, S. V., Yu Mitropol'skaya, S., & Vichuzhanin, D. I. (2007). *Journal of Physics of Metals and Metallography*, 103(3):311.
- [23]. Kiyotomo Nakata, SaburaTakomure, & IsoMasaoka (1985). *Journal of Nuclear Materials*, 131:53.
- [24]. Amdulla, O. O., Mekhabov, M., Doyama, M., Shimotomai, M., & Sato, E. (1985). *Positron annihilation*, P.C. Jain and R.M. Singru (Eds.), Singapore, p. 602.
- [25]. Seydel, O., Froberg, G., & Wever, H. (1964). *Phys. Stat. Sol. (a)*, 144:69.
- [26]. Ali, A. R., Farid, Z. M., & Ghobrial, F. Z. (1994). *Z. Phys. B*, 94:227.
- [27]. Ghazi-Wakili, K., Tippingu Zimmerann, Ph., & Waeber, W. B. (1990). *Z. Phys. B Condensed Matter*, 79, 39 (1990).
- [28]. Dimitrov, O., & Dimitrov, C. (1982). *Journal of Nuclear Materials*, 105:39.
- [29]. Mantl, S., Sharma, B. D., & Antesberger, G. (1979). *Phil. Mag A*, 39:389.
- [30]. Schindler, A. I., Kernohan, R. H., & Weertman, J. (1964). *J. Appl. Phys.*, 35:2640.
- [31]. Seeger, A., & Kronmuller, M. (1987). *Mater. Sci. Frorum.*, 15118:65.
- [32]. Sharma, B. D., Sonnenberg, K., & Antesberger, G. (1985). *Phil. Mag.*, 377:777.
- [33]. Nakata, K., Takamura, S., & Masasak, I. (1985). *Journal of Nuclear Materials*, 131:35.
- [34]. Cullity, B. D. (1972). *Introduction to magnetic materials*. Addison-Wesley Publ. Co., p. 357.
- [35]. Wagenblast H., & Damask, A. C. (1962). *J. Phys. Chem. Solids*, 33:221.
- [36]. Ghazi-Wakili, K., Zimmermann, U., Bruneer, J., Tipping, Ph., Waeber, W. B., & Heinrich, F. (1987). *Phys. Stat. Sol. (a)*, 102:153.
- [37]. Jiles, D. C. (1988). *Phys. Stat. Sol (a)*, 108:417.

